Sigma J Eng Nat Sci, Vol. 43, No. 4, pp. 1211–1223, August, 2025

Sigma Journal of Engineering and Natural Sciences
Web page info: https://sigma.yildiz.edu.tr
DOI: 10.14744/sigma.2025.00115

Research Article

Comparative analysis of aluminum alloys and cast iron as materials for air-cooled internal combustion engines

Jeremiah Lekwuwa CHUKWUNEKE[1,*], Steven Emenike ATUEGBUNAM[1], Victor Ikenna OKORO [2], Kingsley Chidi NNAKWO[3], Onyemazuwa Andrew AZAKA[1], Henry Chukwuemeka OLISAKWE[1], Okechi Lubee EMEANA[1]

[1]Department of Mechanical Engineering, Nnamdi Azikiwe University, Awka, 42000, Nigeria
[2]Department of Mechanical Engineering, Imo State University, Imo, 460222, Nigeria
[3]Department of Metallurgical & Materials Engineering, Nnamdi Azikiwe University, Awka, 42000, Nigeria

ARTICLE INFO

Article history
Received: 28 May 2024
Revised: 24 June 2024
Accepted: 26 July 2024

Keywords:
Air-Cooled Materials; Aluminum Alloys; Cast Iron; Comparative Analysis; Internal Combustion Engines; Modeling and Simulation

ABSTRACT

This paper compares aluminum alloys with cast iron as materials for air-cooled internal combustion engines. Air-cooled internal combustion (IC) engine concept models were developed. The heat exchange characteristics (HECs) of engine models were investigated using the finite element method (FEM). The factors that contribute to low cooling capacity and overall underperformance of air-cooled internal combustion (AIC) engines were investigated using engine models. Thermo-physical properties of engine/fin materials, as well as other parameters such as fin array layout and ventilation speed, have been identified as critical determinants of an AIC engine's HECs. The thermal performance of aluminum alloy and grey cast iron used as alternate engine/fin materials was compared while the engine was first run under natural convection and then at various wind speeds. It was discovered that the high thermal conductivity of the aluminum engine benefits its HEC performance. In contrast, the cast-iron engine benefits from the materials' low specific heat capacity. The thermal analysis also revealed that heat transfer through the cast iron engine section was characterized by a long transient period and a high level of engine heat insulation from the environment, making it a preferred engine option for lightweight stationary machines operated under natural convention. The cooling performance of the engine models was evaluated in terms of fin efficiency and effectiveness. Considering a 175cc engine with a four-fin configuration, comparable global fin efficiencies of useful value 97.42% and 98.65% were obtained for the cast iron engine and aluminum engine, respectively, indicating that heat diffusion to the surroundings was highly efficient in both cases of engine material. Similarly, the fin's effectiveness (ε) was found to be 2.27 and 2.30 for cast iron and aluminum engines, respectively. These ε values are close to the critical value of 2.0, making them less practical. Increasing the number of fins to seven resulted in a significant 42% increase in HECs, reaching a desirable value of ε in both cases of comparable engine materials.

Cite this article as: Chukwuneke JL, Atuegbunam SE, Okoro VI, Nnakwo KC, Azaka OA, Olisakwe HC, Emeana OL. Comparative analysis of aluminum alloys and cast iron as materials for air-cooled internal combustion engines. Sigma J Eng Nat Sci 2025;43(4):1211–1223.

***Corresponding author.**
*E-mail address: jl.chukwuneke@unizik.edu.ng

This paper was recommended for publication in revised form by Editor-in-Chief Ahmet Selim Dalkilic

Published by Yıldız Technical University Press, İstanbul, Turkey

INTRODUCTION

In IC engines, the expansion of high-pressure gases produced during fuel combustion applies a direct force to some components of the engine such as; pistons, turbine blades, or nozzles. This force moves the component over a distance, generating useful mechanical energy. When the combustion of air-fuel mixture takes place in the engine cylinder, a high temperature in the range of over 2000˚C is reached [1-2]. To withstand such a high temperature a very high melting point material has to be used for construction of IC engine. This is practically less possible to achieve, not even with platinum, which has one of the highest melting point values just above 1800˚C [3-4]. When a moving gas comes into contact with a wall, a relatively stagnant gas layer within the boundary layer serves as a thermal insulator [4-5]. The stagnant layer's resistance to heat flow is high. The cylinder gases transfer heat to the cooling medium via this layer and the cylinder walls. A significant temperature drop occurs in the stagnant layer adjacent to the walls. The peak cylinder gas temperature may be 2800 K, but the temperature of the cylinder's inner wall surface may be only 450 K due to cooling [1,6].

Previous research in this field has shown that IC engines can only convert 25-35% of total chemical energy into useful work [7]. Exhaust gases carry approximately 40% into the atmosphere during exhaust stroke. The remainder is also released into the atmosphere via the cooling system [8-10]. The two basic types of cooling systems for IC engines are water-cooling and air-cooling. To achieve a satisfactory result in motor vehicles powered by IC engines, the two cooling methods are typically applied simultaneously using a special device known as a radiator unit [11-13]. In a typical air-cooled IC engine, one common method for controlling excessive temperature rise is to adapt cooling fins on the external surface [14-15]. Cooling fins on an air-cooled IC engine are projected heat transfer surfaces created on the engine's external surface to facilitate heat diffusion from the engine components and affect cooling [16-17]. The use of cooling fins in IC engines improves the engine's thermal efficiency and extends the life of the components by maintaining normal operating conditions, preventing engine seizure/partial meltdown (or welding) of engine components caused by overheating, and reducing thermal fatigue caused by high-temperature fluctuations.

According to reports, the performance of cooling fins in a functional IC engine is affected by several factors, including the number of fins, fin pitch/geometry, surface area of the fin, air-flow rate around the fin, thermal properties of the fin material, and ambient temperature [18-20]. Due to heat accumulation in a functional IC engine and the impact of the environmental factors already identified in the preceding list, the performance of cooling fins initially operating under normal conditions may degrade significantly after a prolonged working period [21-22]. This is more likely to occur in stationary machines, which cause a gradual change in the environment during operation. As a result, high-capacity IC engines suitable for driving heavy equipment machines/vehicles and stationary industrial machines require a more reliable cooling system [23-24]. Most of them use the integrated water channel connected to either a heat exchanger (radiator) unit or a water reservoir. Although these alternative IC engine cooling solutions are already known and well-practiced, the compact nature and economy of fin cooling system make it a preferred cooling technology for lightweight IC engines. However, a low rate of heat transfer through the fins is identified as the main problem in this type of engine cooling. As new technologies powered by air-cooled IC engines evolve, more research is focused on using updated design/manufacturing methods to improve fin efficiency and overcome current limitations. Some of the conventional design strategies include selecting the optimal number of fins, modulating the fin profile, and creating an effective heat transfer area to allow for optimal heat exchange with the surroundings, among others [25-27].

The designer's primary concern when designing cooling fins for an IC engine is to maintain a normal rate of heat dissipation over a typical working duration. On the one hand, insufficient cooling raises the risk of the engine temperature rising too high, causing the lubricant to dry up and overheat, resulting in partial melting of engine components and engine seizure. On the other hand, overcooling the engine results in low thermal efficiency or total ignition loss [27-29]. The optimal operating temperature for an IC engine is between 150 and 200˚C. Conventional fins may perform poorly in critical working conditions due to uncontrollable natural factors. As a result, in many industrial processes which operate on air-cooled IC engines, the field supervisory engineers usually advice on suitable engine indexing arrangements to reduce the relative engine load, and control temperature rise to achieve an uninterrupted process. In a motor cycle operated with air-cooled engine the heat diffusion through the fins is naturally enhanced by forced ventilation provided by the vehicle motion [30]. With proper design of fins and material selection, significant cooling effects have been achieved for normal operation of small power-generating sets and other equivalent IC engine-powered stationary machines. However, due to the low heat exchange rate of the fins, the majority of stationary machine cylinder fins are still made of cast iron, which can withstand high temperatures, as opposed to competing materials such as aluminum and steel [10,31]. Because of the high internal heat generation, the use of air-cooling systems in heavy IC engines such as those used to power automobiles and large industrial machines is still thought to be impractical. This study proposes a detailed investigation of the optimum heat exchange characteristics of an air-cooled IC engine equipped with cooling fins made of different materials to further advance cooling fin technology and its application in air-cooled IC engines beyond its current limitations. Thus, the present study employs the dynamic

finite element model and the principles of robust parameter design (RPD) to evaluate the heat exchange characteristics of AIC engines.

MATERIALS AND METHODS

Materials

This research involves application of dynamic finite element model to simulate heat transport in an air-cooled internal combustion (AIC) engine made of different materials. The two materials that were applied for the research are those considered as engine/fin materials which include grey cast iron and aluminum alloy. They are virtual engine materials implemented in the finite element model. The thermos-physical properties of these materials utilized in the numerical thermal analysis is shown in Table 1 [32].

Table 1. Material properties

Material properties	Aluminum	Cast iron
Rho (Kg/m^3)	2700	7800
Thermal conductivity, k, (W/mK)	235	53
Specific heat capacity, c, (J/kgK)	900	460
Melting point, (°C)	660	1150-1300

Method for Thermal Analysis

The thermal analysis was tailored to reveal what it takes to operate the AIC engine with a desirable configuration in terms of engine/fin material, number of fins and ventilation speed, in line with the goal of the present research. The finite element method (FEM) was adopted for the thermal analysis in preference expensive to obtain the data required for a thermal analysis of the system, and on the other hand, the limitations of analytical models which also rely on experiments for the input data. The finite element model is a high-order numerical computational model which according to several related reports, has tested accuracy in predicting the experimental data in this field.

Two-Dimensional Formulation of the Dynamic Problem

The theoretical formulation of the finite element model is based on the variational method (differential approach). Figure 1 shows a 2D discrete model of a reduced engine section. The model is discretized using triangular elements. A coarse discrete system is used here to illustrate the solution procedure, having in mind that the accuracy of the of the FEM lies on the order of discretization. Thus, the actual solution to the problem discussed applied a refined discrete system of a full-scale engine, of size 175cc. The actual development of the model and simulation of the heat transfer was implemented on the GUI of PDE toolbox, while post-processing of the results was done on Matlab command window.

The complex engine geometry is simplified to a coupled cylinder wall-fin (or engine block) section. The cylinder block is known to provide up to 90% of the total heat transfer area in AIC engines. The dynamic problem visualized in 2-dimensional space assumes symmetry of the heat transfer process about the orthogonal axes such that further simplification may be achieved in solution steps. The Governing equations for 2-dimensional conduction with convection can be written for the finite element procedure using the following guidelines.

The temperature distribution $T(x,y,t)$ is dependent on both space (x,y) and time, t. The differential equation governing the temperature distribution across the coupled wall-fin surfaces is recalled from Zienkiewicz & Taylor [33] as:

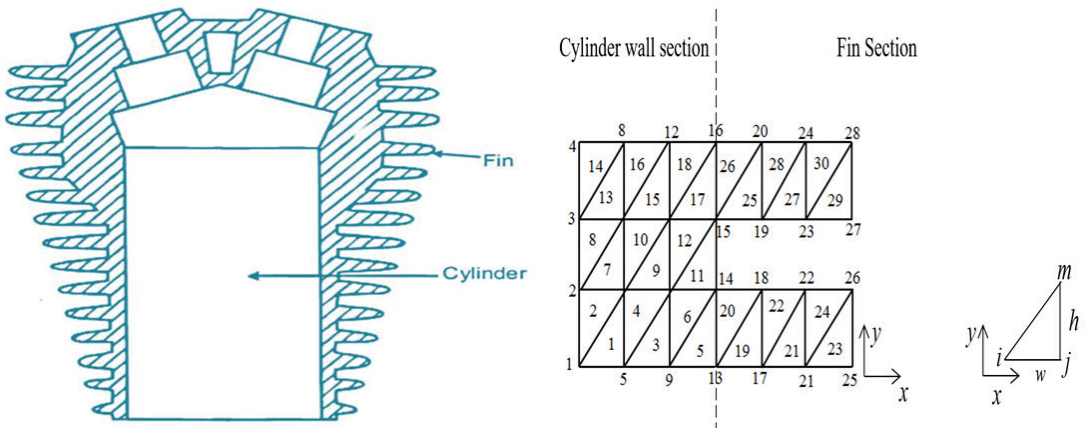

Figure 1. Finite element model of engine cylinder section quipped with cooling fin.

$$k_x \frac{\partial^2 T}{\partial x^2} + k_y \frac{\partial^2 T}{\partial y^2} + Q = \rho c \frac{\partial T}{\partial t} \quad (1)$$

The physical condition and the region considered pose a boundary condition given by;

$$k_x \frac{\partial T}{\partial x} l_x + k_y \frac{\partial T}{\partial y} l_y + q + \alpha T = 0 \quad (2)$$

Where k_x and k_y are the thermal conductivities of the couple engine-fin material; ρ is the density; c is the heat capacity measured at constant pressure; l_x and l_y are the direction cosines of the outward normal to the boundary surface, q represents the heat flux per unit surface and αT is the convection loss. Equation (1) can be re-expressed as Equation (3).

$$\frac{\partial}{\partial x}\left(k_x \frac{\partial T}{\partial x}\right) + \frac{\partial}{\partial y}\left(k_y \frac{\partial T}{\partial y}\right) + Q = \rho c \frac{\partial T}{\partial t} \quad (3)$$

Then, from the principle of variational calculus equivalent formulation of Equation (3) is the requirement that the area integral given as;

$$\chi = \iint \left[\frac{1}{2}\left\{k_x \left(\frac{\partial T}{\partial x}\right)^2 + k_y \left(\frac{\partial T}{\partial y}\right)^2\right\} - \left(Q - \rho c \frac{\partial T}{\partial t}\right) T\right] dxdy \quad (4)$$

The whole computational region should be minimized, subject to the boundary condition. Considering the computational domain as a two-dimensional mapping of the coupled cylinder wall-fin geometry, fully discretized with triangular elements, with the nodes of a typical element labelled *ijm* as shown in Figure 1.

The shape-function which relates the field temperature (T) to the nodal values is expressed as

$$T = \left[N_i, N_j, N_m\right]\{T\}^e \equiv N_i T_i + N_j T_j + N_m T_m \quad (5)$$

where;

$$\begin{aligned} N_i &= \frac{1}{2A}\left[\left(x_j y_m - x_m y_j\right) + \left(y_j - y_m\right)x + \left(x_m - x_j\right)y\right] = \left(a_i + b_i x + c_i y\right)/2A \\ N_j &= \frac{1}{2A}\left[\left(x_m y_i - x_i y_m\right) + \left(y_m - y_i\right)x + \left(x_i - x_m\right)y\right] = \left(a_j + b_j x + c_j y\right)/2A \\ N_m &= \frac{1}{2A}\left[\left(x_i y_j - x_j y_i\right) + \left(y_i - y_j\right)x + \left(x_j - x_i\right)y\right] = \left(a_m + b_m x + c_m y\right)/2A \end{aligned} \quad (6)$$

are the interpolating functions, and

$$\{T\}^e = \left\{T_i, T_j, T_m\right\}' \quad (7)$$

With the nodal values of T defining uniquely and continuously the function all over the region, the functional χ can now be minimized by, first evaluating contributions to each differential such as $\partial\chi/\partial T_i$, for a typical element, then adding all such contributions and equating to zero. Only elements adjacent to node i will contribute to $\partial\chi/\partial T_i$.

Element Equation

Differentiating Equation (4) with respect to the nodal values of temperature

$$\frac{\partial \chi^e}{\partial T_i} = \iint \left\{k_x \frac{\partial T}{\partial x}\frac{\partial}{\partial T_i}\left(\frac{\partial T}{\partial x}\right) + k_y \frac{\partial T}{\partial y}\frac{\partial}{\partial T_i}\left(\frac{\partial T}{\partial y}\right) - Q\frac{\partial T}{\partial T_i} + \rho c \frac{\partial T}{\partial t}\frac{\partial T}{\partial T_i}\right\} dxdy \quad (8)$$

T is defined according to Equation (5) and Equation (6), so that

$$\begin{aligned} &\frac{\partial T}{\partial x} = \frac{1}{2A}\left(b_i, b_j, b_m\right)\{T\}^e, \frac{\partial T}{\partial y} = \frac{1}{2A}\left(c_i, c_j, c_m\right)\{T\}^e, \\ &\frac{\partial T}{\partial T_i} = N_i \text{ and } \frac{\partial T}{\partial t} = \left[N_i, N_j, N_m\right]\left\{\frac{\partial T}{\partial t}\right\}^e \end{aligned} \quad (9)$$

Where; $\frac{\partial T}{\partial t}$ is an invariant.

Combining Equations (8) and (9);

$$\begin{aligned} \frac{\partial \chi^e}{\partial T_i} = {} & \frac{1}{4A^2}\iint \left(k_x\left[b_i, b_j, b_m\right]\{T\}^e b_i + y\left[c_i, c_j, c_m\right]\{T\}^e c_i\right) dxdy \\ & - \frac{1}{2A}\iint Q\left(a_i + b_i x + c_i y\right) dxdy + \iint \rho c N_i \left[N_i, N_j, N_m\right]\left\{\frac{\partial T}{\partial t}\right\}^e dxdy \end{aligned} \quad (10)$$

Every element contributes to only three of the differentials associated with its node such that the results of (10) and of two other similar differentiation are then written in compact form as

$$\left\{\frac{\partial \chi}{\partial T}\right\}^e = \left\{\frac{\partial \chi^e}{\partial T_i}, \frac{\partial \chi^e}{\partial T_j}, \frac{\partial \chi^e}{\partial T_j}\right\}' \quad (11)$$

Or

$$\left\{\frac{\partial \chi^e}{\partial T}\right\} = [h]\{T\}^e + \{F_1\}^e + \{F_2\}^e \quad (12)$$

Since $\frac{\partial T}{\partial t}$ is an invariant, if k_x and k_y are assumed to be constants within the element for homogenous material, then the integration is carried out;

$$\iint dxdy = A(area\ of\ the\ triangle) \quad (13)$$

And

$$[h] = \frac{k_x}{4A}\begin{bmatrix} b_i b_i & b_j b_i & b_m b_i \\ b_i b_j & b_j b_j & b_m b_j \\ b_i b_m & b_j b_m & b_m b_m \end{bmatrix} + \frac{k_y}{4A}\begin{bmatrix} c_i c_i & c_j c_i & c_m c_i \\ c_i c_j & c_j c_j & c_m c_j \\ c_i c_m & c_j c_m & c_m c_m \end{bmatrix} \quad (14a)$$

Or

$$h_{r,s} = \left(k_x b_{r,s} + k_y c_{r,s}\right)/4A \quad (14b)$$

Similarly, if Q is assumed to be constant within the elements, then the vector

$$\{F_1\}^e = -Q\iint (a_i + b_i x + c_i y) dxdy\,/2A \quad (15)$$

Over the area of the triangle, the integral becomes

$$-\left(a_i + b_i \bar{x} + c_i \bar{y}\right)/2 \quad (16)$$

$\bar{x}$ and $\bar{y}$ are coordinates of the centroid given as

$$\bar{x} = (x_i + x_j + x_m)/3 \ and \ \bar{y} = (y_i + y_j + y_m)/3 \quad (17)$$

By substitution, the collection of the integrals for nodes *i,j,m* is found to be

$$\frac{1}{3}\begin{vmatrix} 1 & x_i & y_i \\ 1 & x_j & y_j \\ 1 & x_m & y_m \end{vmatrix} = A/3 \quad (18)$$

And

$$\{F_1\}^e = -QA\{1,1,1\}'/3 \quad (19)$$

Also, the vector $\{F_2\}^e$ can be expressed in a compact form such that the collection of the integral becomes

$$\{F_2\}^e = \iint \rho c[N]^T[N]\left\{\frac{\partial T}{\partial t}\right\}^e dxdy \equiv [\psi]\left\{\frac{\partial T}{\partial t}\right\}^e \quad (20)$$

where,

$$[\psi] = \iint \rho c[N]^T[N]\, dxdy \quad (21)$$

The final assembly equation is then written for individual contribution to the differential system as;

$$\frac{\partial \chi}{\partial T_i} = \sum\sum h_{i,m}T_m + \sum\sum p_{i,m}\frac{\partial T}{\partial t} + \sum F_i = 0 \quad (22)$$

Or for the whole system as

$$[H] + [\psi]\left\{\frac{\partial T}{\partial t}\right\} + \{F\} = 0 \quad (23)$$

This poses a system of linear differential equations of the first order which was solved subject to the boundary conditions using an appropriate time integration scheme, to obtain the instantaneous temperature distribution.

Fin's Efficiency/Effectiveness (Engine Cooling Performance)

The fins are used to force the convective heat transfer from surfaces. The use of fins on a surface cannot be recommended to enhance heat transfer justifies the added cost and complexity associated with the fins. Metrics such as fin's efficiency and fin's effectiveness are used to assess performance of fins in specific applications. Fin's efficiency, η is the ratio between the fin's actual removed heat with the amount of removed heat if all parts of the fin have the same temperature as the fin's base temperature. This matric provides information as to how efficiently on a scale of 1 - 100%, the fin would transfer heat to the surroundings. The value of η depends largely on the thermal properties of the fin material. For AIC engine, useful value of η is expected to be very close to 100%. However, no assurance adding fins to a surface will enhance heat transfer [6]. Thus, the performance of fins is also judged based on the enhancement in heat transfer relative to the no-fin as called fin's effectiveness, ε. The expressions for fin's efficiency, η and fin's effectiveness, ε are written as [34];

$$\eta = \frac{h\sum_{i=0}^{n} A_{si}(T_i - T_\infty)}{h\sum_{i=0}^{n} A_{si}(T_b - T_\infty)} \quad (24)$$

$$\mathcal{E} = \frac{h\sum_{z=0}^{n} A_{si}(T_i - T_\infty)}{hA_b(T_b - T_\infty)} \quad (25)$$

where h is the convective heat transfer coefficient, n is the number of fin's control volume, A_b is the fin base area, A_{si} is the respective surface area of fins, T_b is the instantaneous temperature of the fin base, T_i is the respective instantaneous temperature of fins and T_∞ is the ambient temperature.

The following deductions were made from the fin's performance relations above for consideration in the design and selection of the fins; thermal conductivity (k) of the fin material should be as high as possible. Hence, the most popular fin material is probably aluminum because of its high conductivity, low cost, lightweight and corrosion resistance; the ratio of the perimeter to the cross-sectional area of the fin p/A should be as high as possible. This criterion is satisfied by thin plate fins and slender pin fins, and the use of fins is most effective in applications involving a low convection heat transfer coefficient. This explains the reason fins are placed on the gas side in a liquid-to-gas heat exchanger such as the car radiator. The use of fins is better justified when the transport medium is a gas instead of a liquid and the heat transfer is by natural convection.

The cooling performance of air-cooled internal combustion engine is evaluated in this study in terms of the global fin efficiency/effectiveness. For most practical cases, the value of η is expected to be sufficiently close to 100% while that of ε is often desired to be as high as possible.

RESULTS AND DISCUSSION

Implementation of the Finite Element Model

The heat transfer analysis via the FE model was implemented on PDE toolbox GUI (graphical user interface) and Matlab command window. The GUI facilitates both the preprocessing of a 2D finite element model of the proposed AIC engine as shown in Figure 2 and the numerical solution. However, the raw results of the thermal analysis stored in the PDE toolbox database were in the course of the analysis, exported to the Matlab command window where most post processing of the results were carried out.

The inner wall temperature of the cylinder liner (which exchanges heat first, by convection with hot gas inside the cylinder through the boundary layer, secondly by radiation

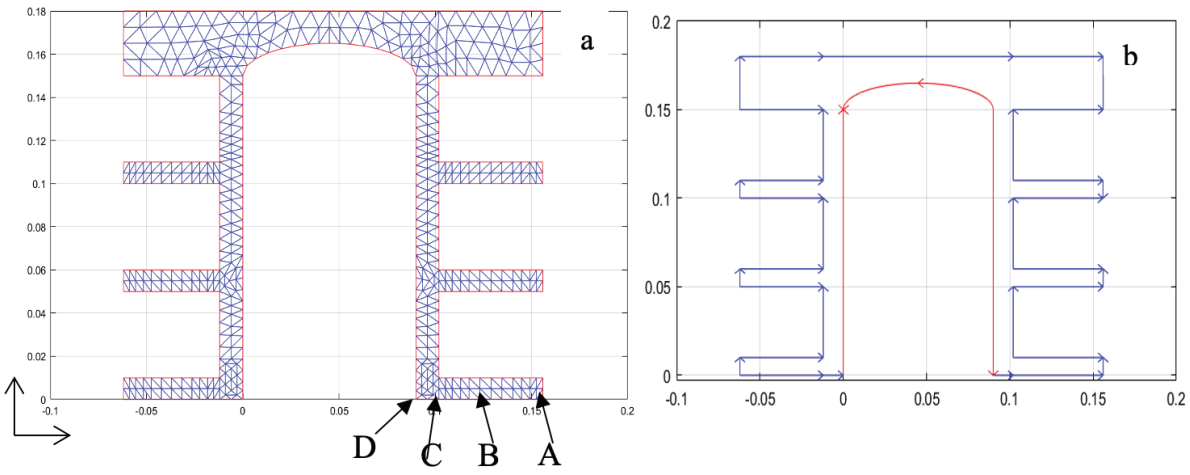

Figure 2. Finite element model of the proposed AIC engine vied in; (a) mesh mode and (b) boundary mode (*Four nodes: A, B, C, and D*).

with hot carbon soot in the combustion chamber and also by conduction with the inner layers of the engine section) was fixed at 200 °C. To all intents and purposes, this value satisfies the typical working condition for AIC engine as discussed in literature [6,8,35]. Thus, a Dirichlet boundary condition (T = 200 °C) was set at the inner wall of the engine section. On the other hand, the outer surfaces of the engine exchanges heat by; conduction with the inner layers of the engine section and convection with the surrounding air whose temperature was assumed to be 27 °C. This pose a Newman boundary condition which was set for the external surfaces according to Equation (2). The entire solution domain was discretized using triangular elements. The results are presented in both mesh and boundary modes in Figures 2(a) and 2(b) respectively. The boundary conditions served as the input to the solution matrix of the simulation model. Preliminary results of the thermal analysis were gathered as discussed in the following sections.

Temperature Distribution

The initial step in the analysis of the heat exchange characteristics (HECs) of the AIC engine involved determination of the instantaneous temperature distribution over the engine sections. First, the case of an all-cast iron engine of size 175cc, equipped with four fins exchanging heat with quiescent air was considered. The color maps of instantaneous temperatures recorded over the solution space were sorted for some specific working durations as shown in Figures 3(a -d).

The overall trends show that while the inner wall of the cylinder liner maintained maximum temperature of 200 °C at all time with temperature rate of 185 to 200 °C, the other layers witnessed initial exponential rise in temperature before they attained a quasi-steady state after a certain period. Later investigation reveals that the length of time it takes to reach a steady state is significantly different for different engine material and depends on the thermal properties of the engine material. The results obtained for the cast iron engine used for the preliminary study indicate that steady state was attained after running the system for about 12 minutes.

Effect of Engine Material

Heat transfer within the engine sections occur by conduction (molecular motion) [36-37]. The heat conduction process is affected by the thermal properties of the engine material such as thermal conductivity, heat capacity and density. To demonstrate the effects of engine material on HECs of the engine, numerical simulation of the heat transfer process was repeated for an equivalent all-aluminum engine and the results were compared with that of grey cast iron. Aluminum alloys as alternative commercial engine materials have significantly different thermo-physical properties from grey cast iron as shown in Table 1, which allows for effective comparative analysis. Four nodes selected along the lower fin labeled 13(A), 120(B), 30(C) and 32(D) in the local/global node numbering system as shown in Figure 2(a) were considered as reference points for the analysis. The results obtained at these points are sufficiently close to those of the corresponding points in the other parts of the engine section. The instantaneous temperature obtained at the reference nodes are presented in Figure 4.

Comparing Figures 4(a) and 4(b), there are clear indications that the material the engine is made of has a significant effect on both the transient and the steady state nodal temperature histories. Aluminum engine witnessed a more rapid rise in temperature within the transient period leading to quicker attainment of a quasi-steady temperature. At the steady state, the temperatures of these nodes were

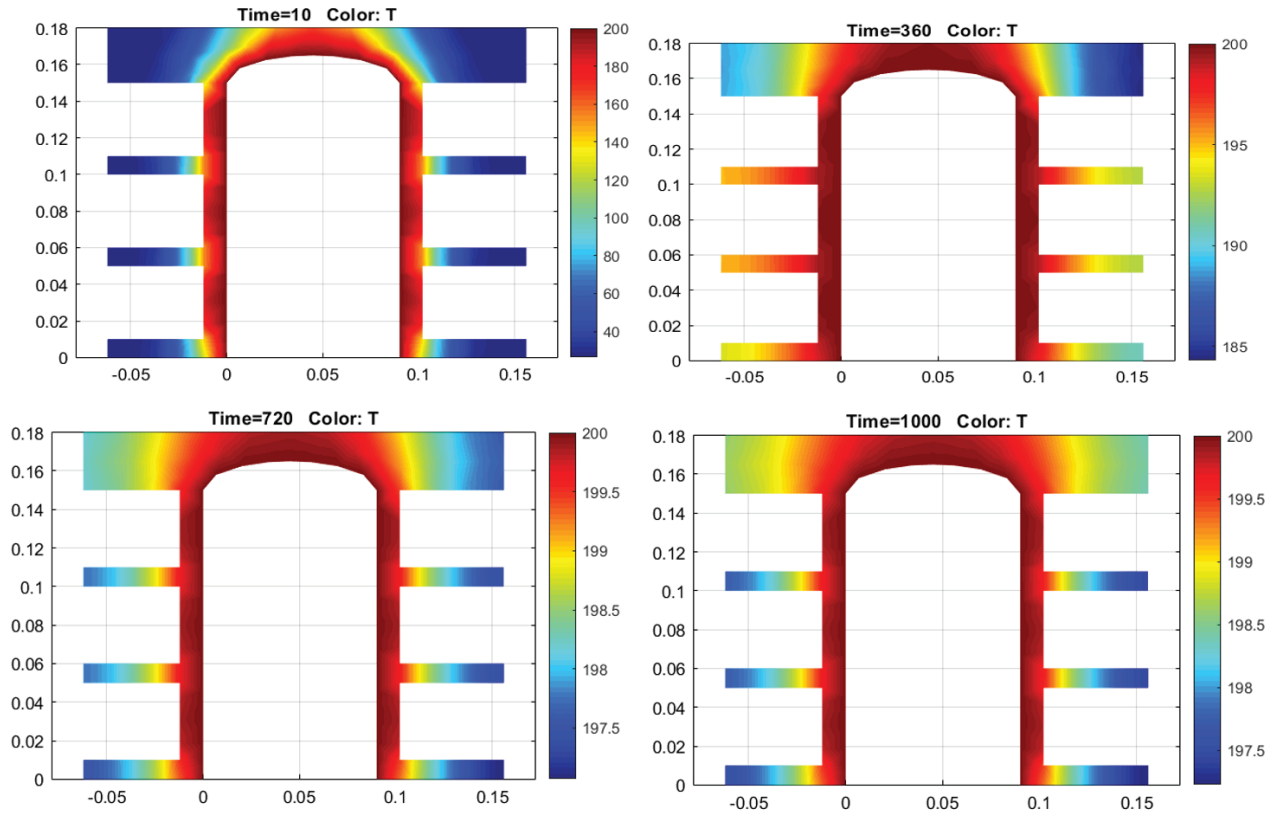

Figure 3. Instantaneous temperature distribution for a 4-fin cast iron AIC engine.

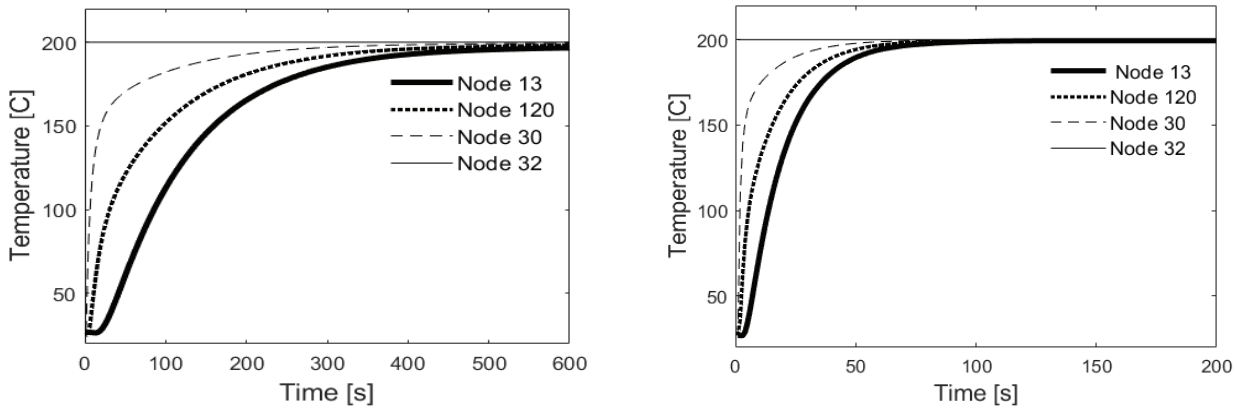

a) b)

Figure 4. Temperature profile obtained at; Node 13, Node 120, Node 30, and Node 32 compared between: (a) Grey cast iron and (b) Aluminum engine materials.

very close to the maximum temperature of the heat source. These characteristics could be attributed to high conductivity of aluminum alloys. The rapid rise to a higher steady temperature shown by all parts of the aluminum engine suggests high fin efficiency. Generally, the nodes closer to the heat source recorded relatively high instantaneous temperatures in the transient zone and quicker rise to a steady state. Thus, the material layers closer to the roots of the fins, as well as those within the cylinder liner are exposed to high temperatures for a longer period within a given operation cycle. In this regard, cast iron engine exhibited generally similar behavior to aluminum engines except that the transient period was much longer and the steady temperature of the fin was visibly lower than the maximum (heat source)

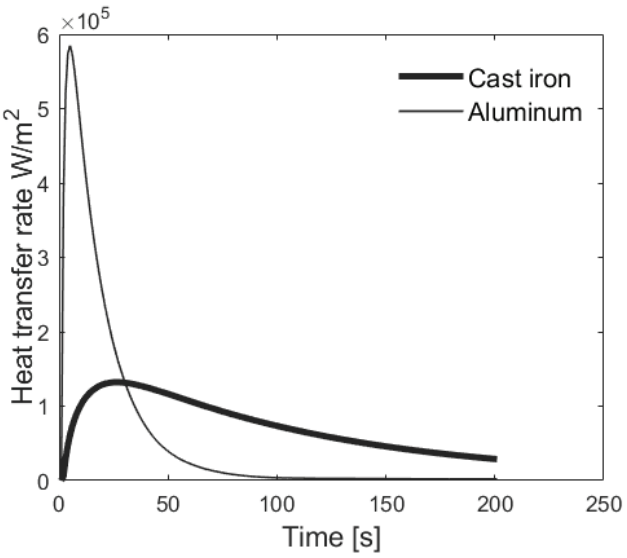

Figure 5. Instantaneous heat flux across the engine fins compared between Grey cast iron and Aluminum engine materials.

temperature. The trends in the result suggest that cast iron material provides significant insulation of the heat from the surrounding even beyond the transient zone, making the steady state heat transfer across the fin to be partly conductive and partly convective, unlike the aluminum engine case where the steady state heat transfer was largely convective.

The effect of the engine material on the heat conduction rate is presented in Figure 5. Aluminum engine showed higher peak heat flux occurring within the transient period and approximately zero heat flux in the steady state. This suggests that at a steady state, all parts of the aluminum engine assume a uniform temperature that is approximately equal to the temperature of the heat source. Thus, temperature gradient between any two reference nodes approached zero at such condition and further heat transport by conduction to or from any part of the engine becomes less feasible. The situation is notably different in the case of the cast iron engine where much lower peak heat flux and apparently non-zero steady heat flux were recorded at the transient and steady state respectively. This suggests that more efficient engine cooling may be guaranteed by aluminum.

However, there is a greater tendency for aluminum engine sections to suffer more material degradation resulting from exposure to higher temperature in a given cycle of operation. Some material degradation associated with prolonged exposure of metallic objects to high temperature such as accumulation of residual stress and modification of surface properties are expected to affect negatively the thermo-mechanical properties of the engine materials, which in turn affect both the operational performance and the durability. The issues around accumulation of stress over a prolonged working period directly affect durability while issues related to the surface properties (roughness or tension) directly affect lubrication and operational efficiency. Thus, in a holistic design consideration, it may not be appropriate to rely on high and absolute convection heat loss guaranteed by aluminum to achieve efficient engine cooling, ignoring the consequences of the inherent high steady temperature. This explains the reason most stationary machines (where forced ventilation is not applicable) are preferably equipped with cast iron engine, and exclusive air-cooling system is not a preferable choice for running heavy equipment or industrial machines.

Effect of Air Ventilation Speed

The impact of the velocity of air flow around the engine was examined for both the heat conduction process through the engine section and the convection heat transfer to the surrounding. The temperature response of the exterior node of the lower fin (Node 13) which seems to be most affected by air flow was utilized for this purpose.

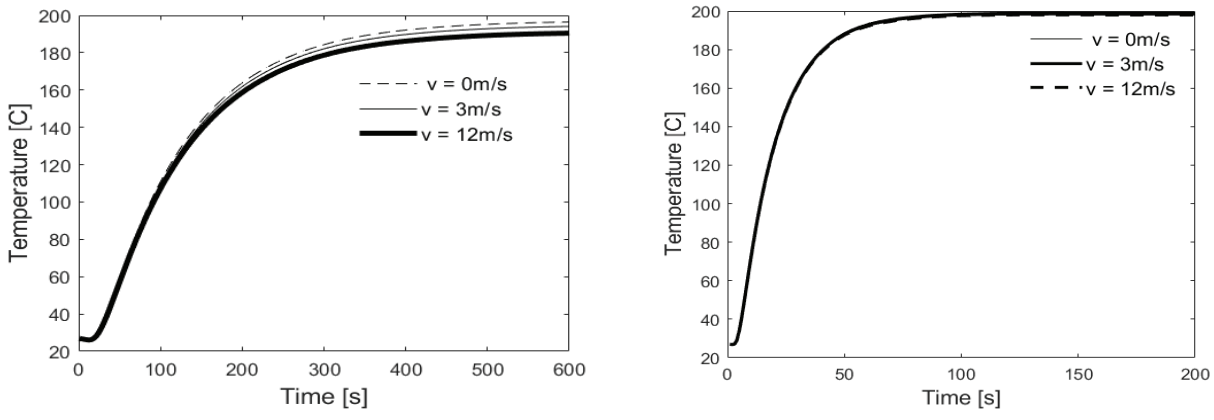

Figure 6. Temperature profiles recorded at Nodes 13 compared between: (a) Grey cast iron and (b) Aluminum engine materials at different air velocities.

The results obtained in the conduction phase are compared between the cast iron engine and aluminum engine in Figures 6(a) and 6(b). Cast iron provides a certain level of insulation of the heat, especially in the early period of heat transfer, to allow for extended heat transfer by both conductions through the engine sections.

Moreover, given to increased convection heat loss at the fin tip associated with high-speed flow, the steady state temperature of the cast iron engine was visibly reduced at higher velocities of air flow as shown in Figure 6(a). Thus, the temperature gradient between the heat source (which is at constant temperature) and the heat sink, as well as the heat conduction rate would invariably increase in the same line according to Fourier law, leading to improved cooling. However, beyond flow speed of about 3m/s, the effect of flow speed vanished progressively. This suggests that in the current application, there is a limit to which increasing velocity of air flow improves the system, with respect to the effectiveness of the engine cooling. On the other hand, heat conduction through the aluminum engine section was not visibly affected by the speed of air flow around the engine (Fig. 6b). This may be attributed to high conductivity of aluminum alloys.

The effects of air flow velocity on the rate of convection heat transfer to the surrounding were also quantified as shown in Figures 7(a) and 7(b) for the cast iron engine and the aluminum engine respectively.

Evidently, convection heat loss in both cases of engine material are quite comparable. The effects of air flow speed on the convection heat transfer rate were very significant and consistent in both cases of engine material as shown in Figure 7. The results indicate that that it is possible to double the heat transfer rate by convection recorded at still air condition by introducing a ventilation speed of 3m/s.

Effect of Number of Fins

To illustrate the effect of the number of fins on the heat exchange characteristics of AIC engine, two variants of the cast iron engine section were drawn to differ by the number of fins only: one with 4 rectangular fins while the other has7 fins of the same dimension. The heat exchange characteristics of the duo was studied, assuming quiescent air condition. The results presented in Figure 8 show in color maps, the steady state temperature distribution of the cast iron engine section compared between the 4-fin array and 7-fin array. Evidently, the 7-fin array provided a wider area for heat transport. The details to the effects of the number of fins are discussed under the following subheadings.

Effect of Number of Fins on the Temperature Profile

For this purpose, instantaneous temperature distribution of the engine was evaluated at Node A, Node B and Node C. The results presented in Figure 9 indicate that while the instantaneous temperature of interior nodes close to the heat source (Node C), including those located between the cylinder liner and the fin base were apparently unaffected by a change in the number of fins in both cases of cast iron and aluminum engine section, a change in the number of fins from 4 to 7 caused significant fluctuation of transient temperature of the fins [see Figures 9(a) and 9(b)].

Effect of Number of Fins on Heat Conduction and Convection

Again, quiescent air condition was considered at this stage to normalize the effects of airflow speed. The conduction phase analysis accounted for the rate of heat transfer from the base (Node C) to the tip of the fin (Node A), while the convection analysis covered heat loss from the tip of the fin (Node A) to the surrounding. The change in number of fins was found to have a very marginal effect

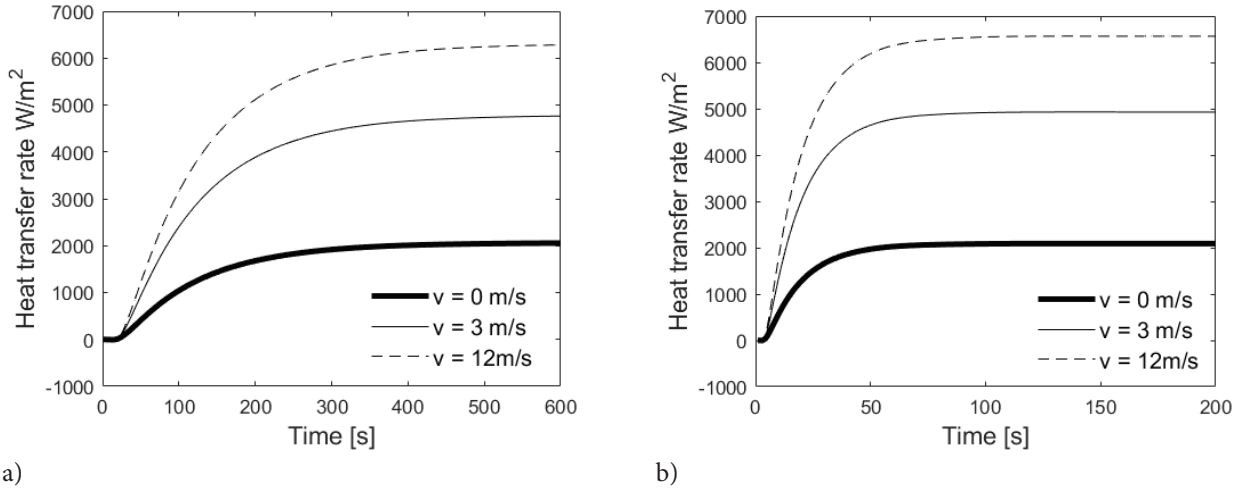

Figure 7. Convection heat transfer rate at various air flow velocities compared between: (a) Grey cast iron engine and (b) Aluminum engine.

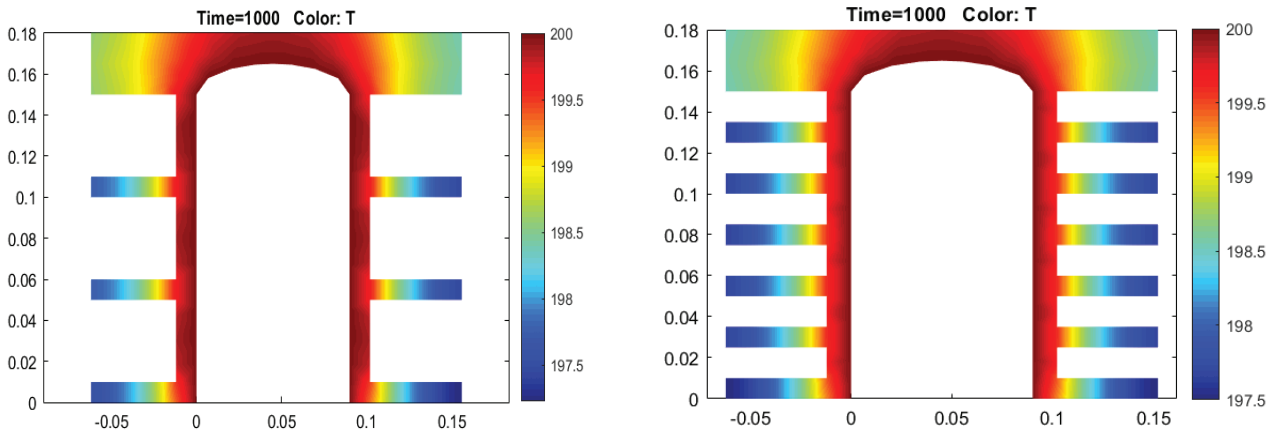

a) b)

Figure 8. Steady state temperature profile evaluated for the cast iron engine sections equipped with: (a) 4 fins, (b) 7 fins.

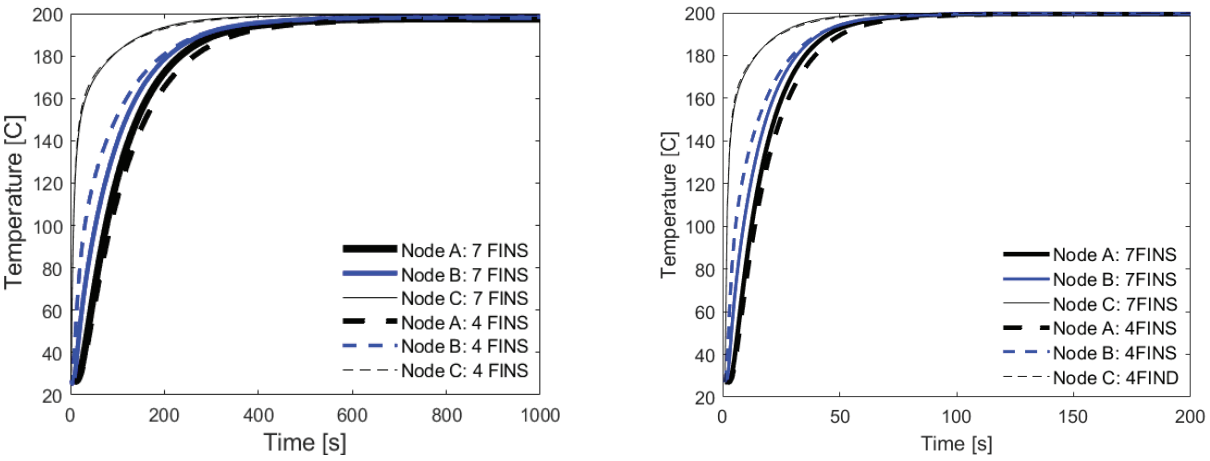

a) b)

Figure 9. Effect of number of fins on temperature histories evaluated at Node A, Node B and Node C of the lower fin for; (a) cast iron engine section and (b) aluminum engine section.

on the transient heat flux in the conduction phase which tends to vanish at a steady state in both cases of aluminum and cast-iron engine sections. The 7-fin array configuration produced relatively lower peak heat flux, though with very little margin (Fig. 10).

The rate of heat transfer in the convection phase was found to be highly separated from that of the conduction phase, thus the duo was compared on a log scale separately for 4-fin array and 7-fin array configurations in Figures 11 and 12 respectively.

The comparative study reveals that although the two studied engine materials applied to any of the alternative fin configurations guarantee apparent convergence to a common steady heat transfer rate of about 2000W/m^2, yet a closer look at the results reveals that with the 4-fin array, the steady convection heat transfer rate was slightly lower than the steady conduction heat transfer rate (see Figure 11), while in the 7-fin array, the reverse was the case (see Figure 12). The latter case in which the rate of convection heat loss to the surroundings exceeds the heat conduction rate across the fins at steady state suggests a better cooling effect.

Cooling Performance Analysis

Cooling performance of the engine was evaluated at various configurations in terms of the global fin's efficiency, and the global fin's effectiveness using Equations (24) and (25) respectively. The comprehensive result is presented in Table 2.

Total surface area of engine without fin, $A_b = 0.1608m^2$; Total surface area of the engine with η number of fins is

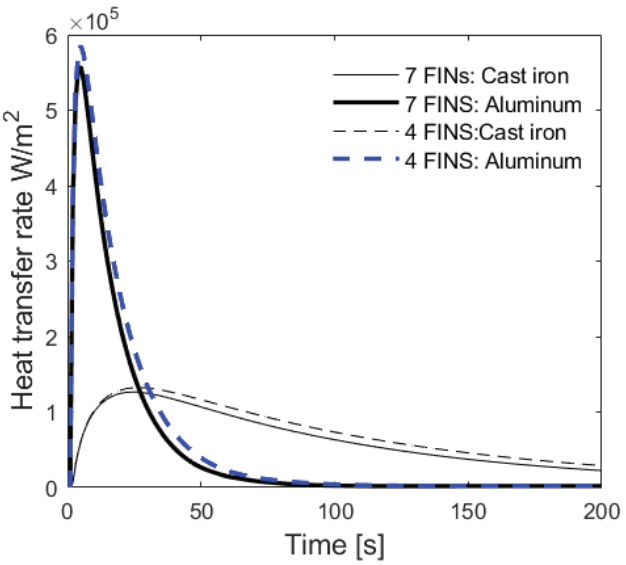

Figure 10. Instantaneous rate of heat transfer by conduction across the fins compared between 7-fin array and 4-fin array made of different materials.

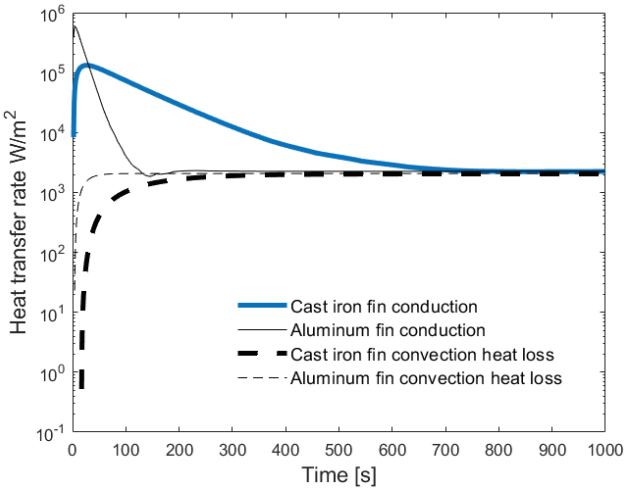

Figure 11. Conduction heat transfer rate through the fin compared to the rate of convection heat loss to quiescent atmosphere for the 4-fin array.

given by; $A_{f,n} = A_b + (n - 1)A_{f2} + A_{f1}$ from which; $A_{f,4} = 0.3709m^2$, $A_{f,7} = 0.5275m^2$ were obtained.

We recalled that fin's effectiveness, ε is the ratio between the fin's actual removed heat with the amount of removed heat if a fin is uninitialized [38]. Thus, the global fin's effectiveness was estimated as the ratio of the total convective heat loss through the entire engine surface exposed to the atmosphere, (including the finned and un-finned area), to the equivalent total convective heat loss through the engine surface when the fins were excluded. The desire is to have this ratio as large as possible while keeping the additional cost of adding the fins as low as possible. A fin effectiveness value greater than 2 is a common rule-of-thumb requirement for adding fins to a surface. In other words, fin effectiveness value, $\varepsilon > 2$is usually not acceptable for most practical purposes. We can understand that acceptable fin effectiveness and efficiency were guaranteed for both the

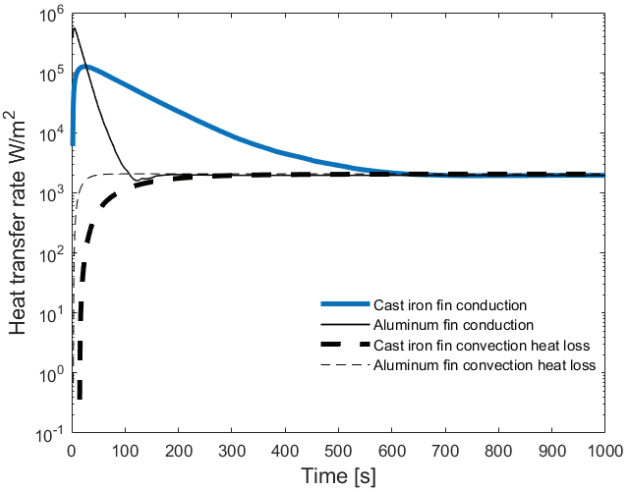

Figure 12. Conduction heat transfer rate through the fin compared to the rate of convection heat loss to quiescent atmosphere for the 7-fin array.

Table 2. Characteristics of conduction/convection heat transfer through the fin evaluated for the various configurations of the engine section

IC engine configuration	Maximum heat flux ($\times 10^5$ W/m^2)	Heat transfer rate obtained at steady state (W/m^2)		Global Fin Effectiveness ε	Global Fin Efficiency η
		Conduction	Convection		
Cast iron engine equipped with 4 fins	1.3236	2240	2042.7	2.2712	97.42
Cast iron engine equipped with 7 fins	1.2653	1960	2046	3.2354	97.58
Aluminum engine equipped with 4 fins	5.8539	2250	2068.5	2.2986	98.65
Aluminum engine equipped with 7 fins	5.5749	1950	2069.2	3.2702	98.69
Cast iron engine without fin	11.4612	-	2074.5	-	-
Aluminum engine without fin	11.4612	-	2075.7	-	-

aluminum and cast-iron engines with a 4-fin array. The trend in the results suggests that lower numbers of fins < 4 for the engine specification may lead to unacceptable cooling performance. Efforts to compare the performance of the alternative engine configurations at higher fin numbers reveal that cooling performance was dramatically improved in the equivalent 7-fin array as shown in Table 2.

CONCLUSION

Heat exchange characteristics of a 175cc AIC engine were successfully studied using the finite element model. The results were analyzed extensively to arrive at the following conclusions:

1. In the design of AIC engines, improved HECs can be achieved for an engine through the following ways;
   - ***Proper material selection:*** Appropriate material for the AIC engine/fin should have high thermal conductivity (as high as possible), low specific heat capacity and guarantee thermal stability at elevated temperature.
   - ***Detailed thermal analysis:*** Detailed thermal analysis (such as the one demonstrated in this thesis) must be conducted to reveal the configuration of the engine that would guarantee a desirable HECS.
   - ***Performance evaluation:*** Cooling performance of the engine/fin should be quantified at the design stage using appropriate performance metric(s) such as fin's effectivity linked to the engine HECS data obtained via a high-order numerical computational model. This ensures that the cooling performance of final product lies within acceptable value.
2. Two similar AIC engines of the size studied in this thesis (one is made of Aluminum alloy while the other is made of Gray cast iron material) operated under natural convection have significantly different instantaneous HECS. Their steady state cooling capacity is quite comparable and acceptable, provided adequate number of fins is applied. This finding justifies the use of the two materials as alternative commercial materials for AIC engines.
3. Cast iron material, due to its relatively low thermal conductivity provides a considerable level of insulation of the heat generated at the combustion chamber. Consequently, the thermal efficiency of the cast iron engine is relatively low, especially in the beginning of the process. This is capable of stopping ignition especially in compression ignition (CI) system with low compression ratio (CR), thus, justifying the use of aluminum alloy as the preferred material for manufacturing the cylinder head and the adoption of spark ignition (SI) system for most AIC engines.

AUTHORSHIP CONTRIBUTIONS

Authors equally contributed to this work.

DATA AVAILABILITY STATEMENT

The authors confirm that the data that supports the findings of this study are available within the article. Raw data that support the finding of this study are available from the corresponding author, upon reasonable request.

CONFLICT OF INTEREST

The author declared no potential conflicts of interest with respect to the research, authorship, and/or publication of this article.

ETHICS

There are no ethical issues with the publication of this manuscript.

REFERENCES

[1] Alam MI, Mujahid AA, Salam B. Computational simulation of IC engine cooling using different materials for different shapes of fins: A comparative study. Int J Ambient Energy 2022;44:147–156. [CrossRef]

[2] Subbiah M, Balamurugan S, Jayakumar K, Karthick R. Analysis of engine cylinder block with fins by varying different materials. Mater Today Proc 2023;72:2039–2043. [CrossRef]

[3] Bharti R. Design Optimization of an Air Cooled Internal Combustion Engine Fin Using CFD. Int J Res Appl Sci Eng Technol 2018;6:70–73. [CrossRef]

[4] Mahajan P, Thakur A, Bodake R. Correlation of experimental thermal mapping and FEA thermal simulation for cylinder head for diesel engine development. SAE Tech Paper Series 2020. http://dx.doi.org/10.4271/2020-28-0353 [CrossRef]

[5] Sahu A, Bhowmick S. Solution of transient heat transfer in graded-material fins of varying thickness under step changes in boundary conditions using the Lattice Boltzmann Method. Heat Transfer 2022;51:4143–4168. [CrossRef]

[6] Sharan KNS, Malla RK, Raju PR, Nikhil K, Krishnan VR. Modelling and Analysis of IC Engine Fins by using Different Materials. Int J Modern Trends Sci Technol 2022;8:188–204.

[7] Mejía-Gallón V, Gomez S, Estrada Grisales D, Fula MA. 6-Stroke water injection engine literature review with an introduction of heat transfer and thermodynamic analysis. Int J Environ Sci Technol 2024;21:6911–6924. [CrossRef]

[8] Nitnaware PT, Giri PS. Design Optimization Of An Air Cooled Internal Combustion Engine Fin Using CFD. J Multidiscip Eng Sci Technol 2015;2:3129–3131.

[9] Srikanth J, Kumar AJ. Modeling and Static Thermal Analysis of IC Engine Piston by using Different Materials. Int J Appl Sci Eng Manag 2017;6:265–272.

[10] Karthikeyan K, Saravanan C, Kumar TS. Enhancement of heat transfer analysis and optimization of engine fins of varying geometry. Int J Trend Sci Res Dev 2018;2:1384–1389. [CrossRef]
[11] Achebe CH, Ogunedo BMO, Chukwuneke JL, Anosike NB. Analysis of diesel engine injector nozzle spray characteristics fueled with residual fuel oil. Heliyon 2020;6:e04637. [CrossRef]
[12] Chukwuneke JL, Achebe CH, Okolie PC, Obiora E, Anisiji OE. Modeling of electromechanical control of camless internal combustion engine valve actuator. Int J Sci Eng Invest 2013;2:123–136.
[13] Chukwuneke JL, Aniemene CP, Okolie PC, Obele CM, Chukwuma EC. Analysis of the dynamics of a freely falling body in a viscous fluid: Computational fluid dynamics approach. Int J Thermofluids 2022;14:100157. [CrossRef]
[14] Srinivas D, Kumar Thalla RS, Suresh V, Eshwaraiah R. Thermal analysis and optimization of engine cylinder fins by varying geometry and material. 1st Intern Conf Manuf Mater Sci Eng (ICMMSE-2019) 2019. http://dx.doi.org/10.1063/1.5141181 [CrossRef]
[15] Rudra Devraj, Chaturvedi S. Optimization of thermal analysis of engine cylinder fins by varying geometry. Int J Sci Res Sci Eng Technol 2023;492–506. [CrossRef]
[16] Kumar S, Diwakar V. Analysis of engine cylinder to optimize heat transfer by varying fin geometry. Smart Moves J Ijoscience 2021;64–69. [CrossRef]
[17] Nain A, Nene D, Unnithan S. Cooling system optimization in an air-cooled CNG engine using 3-D CFD technique. SAE Tech Paper Series 2022. http://dx.doi.org/10.4271/2022-01-0206 [CrossRef]
[18] Rao NPR, Vardhan TV. Thermal Analysis of Engine Cylinder Fins By Varying Its Geometry and Material. Int J Eng Res Technol 2023;2:1694.
[19] Savvakis S, Mertzis D, Nassiopoulos E, Samaras Z. A design of the compression chamber and optimization of the sealing of a novel rotary internal combustion engine using CFD. Energies 2020;13:2362. [CrossRef]
[20] Leach F, Kalghatgi G, Stone R, Miles P. The scope for improving the efficiency and environmental impact of internal combustion engines. Transp Eng 2020;1:100005. [CrossRef]
[21] Kumar A, Gupta AK, Banti, Samsher. Design optimization and computational analysis of heat transfer through IC engine fins. In: Lecture Notes Mech Eng. Springer Singapore; 2021. p. 683–694. [CrossRef]
[22] Mekroud A, Bidi L, Boukebbab S, Boulahlib MS, Chaib R. Establishing thermal balance during the cooling system improvement of an air-cooled engine. Technol Audit Prod Reserves 2023;6:13–20. [CrossRef]
[23] Xiao K, He J, Feng Z. Heat transfer enhancement of swirl cooling by different crossflow diverters. Volume 6B: Heat Transfer — General Interest/Additive Manufacturing Impacts on Heat Transfer; Internal Air Systems; Internal Cooling; 2022. http://dx.doi.org/10.1115/gt2022-82775 [CrossRef]
[24] Sachar S, Parvez Y, Khurana T, Chaubey H. Heat transfer enhancement of the air-cooled engine fins through geometrical and material analysis: A review. Mater Today Proc 2023. https://doi.org/10.1016/j.matpr.2023.03.447 [CrossRef]
[25] Badra J, Khaled F, Tang M, Pei Y, Kodavasal J, Pal P, Owoyele O, Fuetterer C, Brenner M, Farooq A. Engine combustion system optimization using CFD and machine learning: A methodological approach. ASME 2019 Internal Combustion Engine Div Fall Tech Conf 2019. Paper No: ICEF2019-7238, V001T06A007. [CrossRef]
[26] Barua A, Pradhan S, Kumari K, Naik B, Priyadarshini M, Choudhury SK, Panicker RV, Jeet S. Comparative evaluation based on FEA of thermal analysis of IC engine cylinder using different materials. Mater Today Proc 2023;6:13–20.
[27] Abdullah Md, Zoynal Abedin M. Recent development of combined heat transfer performance for engine systems: A comprehensive review. Results Surf Interfaces 2024;15:100212. [CrossRef]
[28] Dahham RY, Wei H, Pan J. Improving thermal efficiency of internal combustion engines: Recent progress and remaining challenges. Energies 2022;15:6222. [CrossRef]
[29] Prajapati S, Mehta N, Thakur AN. Design and analysis of IC engine combustion chamber and piston by composite materials (al & MG) using finite element analysis. Res Square Platform LLC 2022. http://dx.doi.org/10.21203/rs.3.rs-1886165/v1 [CrossRef]
[30] Di Battista D, Cipollone R. Waste energy recovery and valorization in internal combustion engines for transportation. Energies 2023;16:3503. [CrossRef]
[31] Nimal RJGR, Rajalakshmi A. Design and analysis of various material two-wheeler engine cooling fins. Int J Psychosoc Rehabil 2019;23:83–93. [CrossRef]
[32] Karthik S, Muralidharan K, Anbarasan B. Material selection for fin based on thermal analysis using ANSYS and ANN. Int J Mech Eng Technol 2018;9:560–567.
[33] Zienkiewicz OC, Taylor RL. The finite element method for solid and structural mechanics. Butterworth-Heinemann; 2013.
[34] Nugroho TD, Purwadi PK. Fins effectiveness and efficiency with position function of rhombus sectional area in unsteady condition. AIP Conf Proc 2017;1788:1–6. [CrossRef]
[35] Singh R, Singh SP, Singh A. Analysis of IC Engine Air Cooling of Varying Geometry and Material. Imperial J Interdisciplinary Res 2016;2:1–8.
[36] Ghassemi M, Shahidian A. Biosystems heat and mass transfer. In: Nano and Bio Heat Transfer and Fluid Flow. Elsevier; 2017. p. 31–56. [CrossRef]
[37] Sasongko SB, Huang RF, Hsu CM. Effects of backward inclination on a pulsed jet in crossflow. J Wind Eng Ind Aerodyn 2021;214:104662. [CrossRef]
[38] Çengel YA. Heat Transfer A Practical Approach. McGraw-Hill Companies, Inc.; 2008.